Molecular Microbiology (2009) 74(3), 594–608 ■
doi:10.1111/j.1365-2958.2009.06880.x
First published online 30 September 2009

Molecular characterization of staphyloferrin B biosynthesis in *Staphylococcus aureus*

Johnson Cheung,[1] Federico C. Beasley,[1] Suya Liu,[2] Gilles A. Lajoie[2] and David E. Heinrichs[1]*
Departments of [1]Microbiology and Immunology and [2]Biochemistry, University of Western Ontario, London, Ontario, Canada N6A 5C1.

Summary

Siderophores are iron-scavenging molecules produced by many microbes. In general, they are synthesized using either non-ribosomal peptide synthetase (NRPS) or NRPS-independent siderophore (NIS) pathways. *Staphylococcus aureus* produces siderophores, of which the structures of staphyloferrin A and staphyloferrin B are known. Recently, the NIS biosynthetic pathway for staphyloferrin A was characterized. Here we show that, in *S. aureus*, the previously identified *sbn* (siderophore biosynthesis) locus encodes enzymes required for the synthesis of staphyloferrin B, an α-hydroxycarboxylate siderophore comprised of L-2,3-diaminopropionic acid, citric acid, 1,2-diaminoethane and α-ketoglutaric acid. Staphyloferrin B NIS biosynthesis was recapitulated *in vitro*, using purified recombinant Sbn enzymes and the component substrates. *In vitro* synthesized staphyloferrin B readily promoted the growth of iron-starved *S. aureus*, via the ABC transporter SirABC. The SbnCEF synthetases and a decarboxylase, SbnH, were necessary and sufficient to produce staphyloferrin B in reactions containing component substrates L-2,3-diaminopropionic acid, citric acid and α-ketoglutaric acid. Since 1,2-diaminoethane was not required, this component of the siderophore arises from the SbnH-dependent decarboxylation of a 2,3-diaminoproprionic acid-containing intermediate. Liquid chromatography-electrospray ionization-mass spectrometry (LC-ESI-MS) analyses of a series of enzyme reactions identified mass ions corresponding to biosynthetic intermediates, allowing for the first proposed biosynthetic pathway for staphyloferrin B.

Accepted 8 September, 2009. *For correspondence. E-mail deh@uwo.ca; Tel. (+1) 519 661 3984; Fax (+1) 519 661 3499.

Introduction

Iron is an essential, yet limiting, nutrient for virtually all organisms. Iron limitation frequently results from iron existing in the oxidized ferric (Fe^{3+}) form which then reacts with oxygen to form hydroxide and oxyhydroxide precipitates (Barry and Challis, 2009). Bacteria have evolved several means by which to secure iron but, by far, the most common strategy invokes the use of small molecules termed siderophores. Siderophores are low-molecular-weight compounds made of both amino acids and non-proteogenic amino acids (Miethke and Marahiel, 2007). Different types of siderophores exist depending on functional groups involved in iron co-ordination. Siderophores can be synthesized by modular enzymatic platforms called non-ribosomal peptide synthetases (NRPS) which synthesize siderophores using protein carrier-linked intermediates (for a review, see Crosa and Walsh, 2002). The best-characterized NRPS-dependent siderophore is enterobactin. Another enzymatic route to siderophore synthesis is through the NRPS-independent siderophore (NIS) synthetase system which utilizes condensation reactions with units of dicarboxylic acids, diamines and/or amine alcohols to form the final siderophore structure (Challis, 2005). This biosynthetic method differs from the NRPS system in that intermediates and enzymes are freely dissociable from one another during assembly. Aerobactin, produced from *Escherichia coli*, represents the model NIS. Its biosynthesis utilizes two siderophore synthetases, IucA and IucC, to condense two molecules of *N*6-acetyl-*N*6-hydroxylysine to a citrate molecule (de Lorenzo and Neilands, 1986). Due to advances in bioinformatics and microbial genome sequencing, knowledge of NIS systems has expanded tremendously; NIS systems are present in over 40 bacterial species.

In brief, the mechanism of NIS synthetases begins with the ATP-dependent, enzymatic adenylation of a carboxylic acid to form an enzyme-linked acyl-adenylate (Challis, 2005; Schmelz *et al.*, 2009). The intermediate thus formed is reactive and prone to an addition–elimination reaction with a second substrate containing a nucleophilic amino or hydroxyl group to form an ester or amide. A model, based on the characterized functions of IucA and IucC, has been put forth to categorize NIS synthetases into three distinct classes named type A, B and C; the

model proposes that each type of synthetase will recognize a certain carboxylic acid substrate along with an additional amine or alcohol substrate (Challis, 2005). By definition, type A synthetases will catalyse formation of an amide (or ester) bond between an amino or hydroxyl group containing substrate and one of the two prochiral carboxylic acids of citrate. Type B synthetases are thought to recognize the C5 carboxyl portion of α-ketoglutarate (α-KG) and will condense it to amino or hydroxyl functional groups on a second substrate to form amide or ester bonds respectively. Lastly, type C synthetases will catalyse the amide or ester bond formation between a substrate with an amino or hydroxyl group with a second substrate which is already a monoamide or monoester that still has a free prochiral carboxyl group.

Staphylococcus aureus is a notorious Gram-positive bacterial pathogen. It is the causative agent of a large number of maladies, ranging from impetigo and skin abscesses to more serious infections including pneumonia, food poisoning, endocarditis, meningitis, toxic shock and septicaemia. Members of the staphylococci produce two structurally characterized polycarboxylate-type siderophores called staphyloferrin A (SA) and staphyloferrin B (SB) (Konetschny-Rapp *et al*., 1990; Meiwes *et al*., 1990; Drechsel *et al*., 1993; Haag *et al*., 1994). Production of SA, composed of D-ornithine and two molecules of citrate, requires the activity of the *sfa* gene products (Beasley *et al*., 2009; Cotton *et al*., 2009). Synthesis of the δ-citryl-D-ornithine intermediate requires SfaD whereas condensation of this intermediate to another molecule of citrate to produce the final siderophore structure is carried out by the activity of SfaB (Cotton *et al*., 2009). It is presumed that in the cell, D-ornithine is produced by the activity of a putative ornithine racemase (SfaC).

Staphylococcus aureus possesses a second genetic locus (*sbnA–I*) responsible for siderophore production. Insertional inactivation of *sbnE* or deletion of the entire nine-gene *sbn* operon eliminates production of a siderophore and results in decreased growth in iron-starved media (Dale *et al*., 2004a; Beasley *et al*., 2009). In *S. aureus*, the locus has not yet been linked to synthesis of a particular structurally characterized siderophore but deletion of a homologous locus in *Ralstonia* spp. resulted in loss of SB in iron-starved culture supernatants (Bhatt and Denny, 2004), lending support to the hypothesis that *sbn* in *S. aureus* is responsible for production of SB. Synthesis of SB, which contains L-2,3-diaminopropionic acid (Dap), citrate, 1,2-diaminoethane (Dae) and α-KG (Drechsel *et al*., 1993), is predicted to require the activity of three NIS synthetase enzymes to condense these substrates. The *sbn* gene locus encodes three such NIS synthetases, SbnE, SbnC and SbnF, which are classified as type A, type B and type C siderophore synthetases respectively. Thus, it was reasonable to assume that SB synthesis required the products of the *sbn* gene locus.

Herein, we report the first molecular and biochemical characterization of SB biosynthesis. We show that production of SB in iron-starved culture supernatants of *S. aureus* is dependent on the presence of the *sbn* locus. Sbn enzymes were overexpressed, purified and characterized for their specific activity. The results demonstrate that the minimal SB synthetase consists of SbnCEF, with the added requirement of the decarboxylase enzyme SbnH. Accordingly, substrate specificity and electrospray ionization-mass spectrometry (ESI-MS) results of these enzymes and their reaction products allow us to propose for the first time the biosynthetic pathway for the siderophore. We further demonstrate that SB, synthesized *in vitro*, is able to supply the iron needs of *S. aureus* in a SirABC transporter-dependent manner.

Results

The S. aureus sbn *operon is associated with production of staphyloferrin B*

Staphylococcus aureus strains Newman and RN6390 produce the siderophore SA under iron starvation growth conditions (Beasley *et al*., 2009), and the genetic determinants (a four-gene locus, *sfaA–D*) for SA biosynthesis in *S. aureus* were recently identified and characterized (Beasley *et al*., 2009; Cotton *et al*., 2009). Analysis of deletion mutants demonstrated that in strains RN6390 and Newman, siderophore production was determined by two genetic loci – the aforementioned *sfa* locus as well as the previously described, nine-gene *sbn* operon (Dale *et al*., 2004a; Beasley *et al*., 2009) (Fig. 1A). Given that mutations in the orthologous gene cluster in *Ralstonia solanacearum* and *R. metallodurans* result in the loss of SB (Bhatt and Denny, 2004) (Fig. 1B), it was reasonable to hypothesize that products of the *sbn* operon in *S. aureus* synthesize SB. Therefore, iron-starved spent culture supernatant from *S. aureus* H1661 (RN6390 Δ*sfa*) (note: a SA-deficient genetic background was used to simplify siderophore extraction and analysis) was analysed for the presence of SB, and compared with that of *S. aureus* H1649 (RN6390 Δ*sfa*Δ*sbn*). As illustrated in Fig. 2, SB ($[M\text{-}H]^- = 447.14$) was detected in the iron-starved spent culture supernatant of H1661, but not H1649, confirming that the *sbn* operon is involved in the synthesis of this siderophore. Previous results demonstrated that culture supernatants of H1661, but not H1649, could promote the iron-starved growth of *S. aureus*, as would be expected should H1661 synthesize a molecule with siderophore properties (Beasley *et al*., 2009).

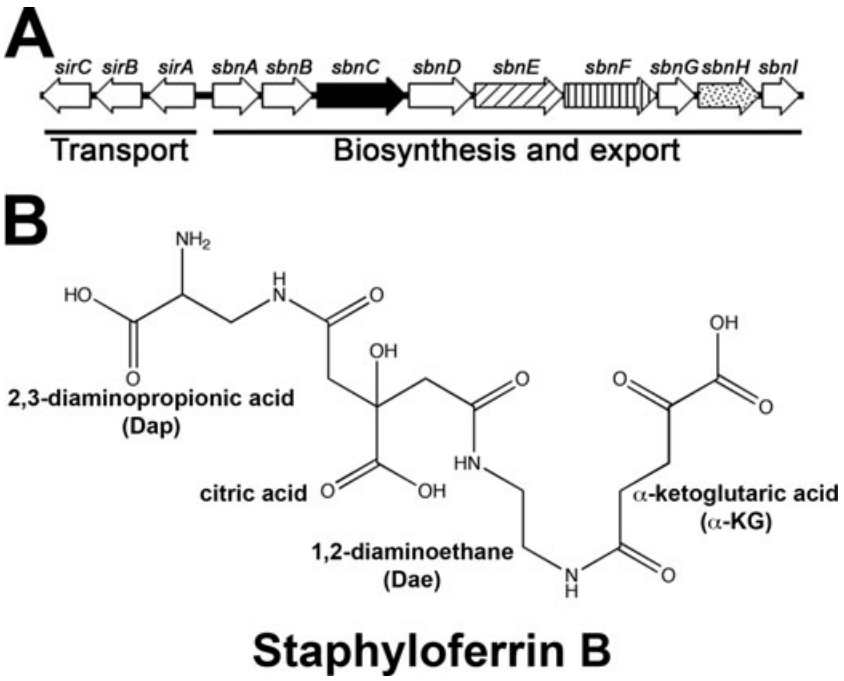

Fig. 1. A. Physical map of the *S. aureus sir-sbn* genetic locus. Predicted products highlighted are type A (angle lines), type B (solid) and type C (vertical lines) NIS synthetases and a decarboxylase (dotted). B. Structure of staphyloferrin B. Components of the siderophore are indicated.

In vitro *synthesis of staphyloferrin B requires three NIS synthetases (SbnCEF) and a decarboxylase (SbnH)*

Bioinformatic analyses of the predicted protein products from the SB biosynthesis operon identified three enzymes (SbnC, SbnE and SbnF) that belong to the NIS family of siderophore synthetase enzymes. From previous studies, it is known that these enzymes catalyse the ATP- and Mg^{2+}-dependent activation of carboxylate substrates, in a reaction that proceeds through an acyl-adenlyate intermediate that is then recognized by an amine substrate to yield a condensation reaction forming an amide (Oves-Costales *et al.*, 2007; 2008; Berti and Thomas, 2009; Cotton *et al.*, 2009; Kadi and Challis, 2009). To examine

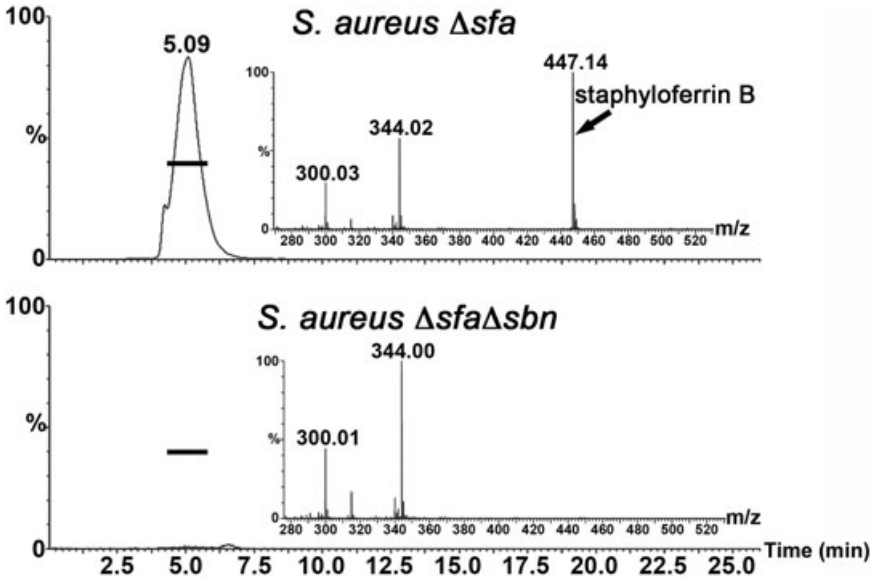

Fig. 2. Identification of staphyloferrin B production by *S. aureus* RN6390. Top panel: Concentrated spent culture supernatant from iron-starved *S. aureus* RN6390 *sfa* was subjected to LC-ESI-MS analysis. Shown is the selected ion chromatogram for the ion at *m/z* 447.1 from LC-ESI-MS and the ESI-MS spectra (inset) of the region in the chromatogram indicated by the horizontal black bar. Bottom panel: Same as the top panel but material was obtained from an iron-starved *S. aureus* RN6390 Δ*sfa*Δ*sbn* mutant.

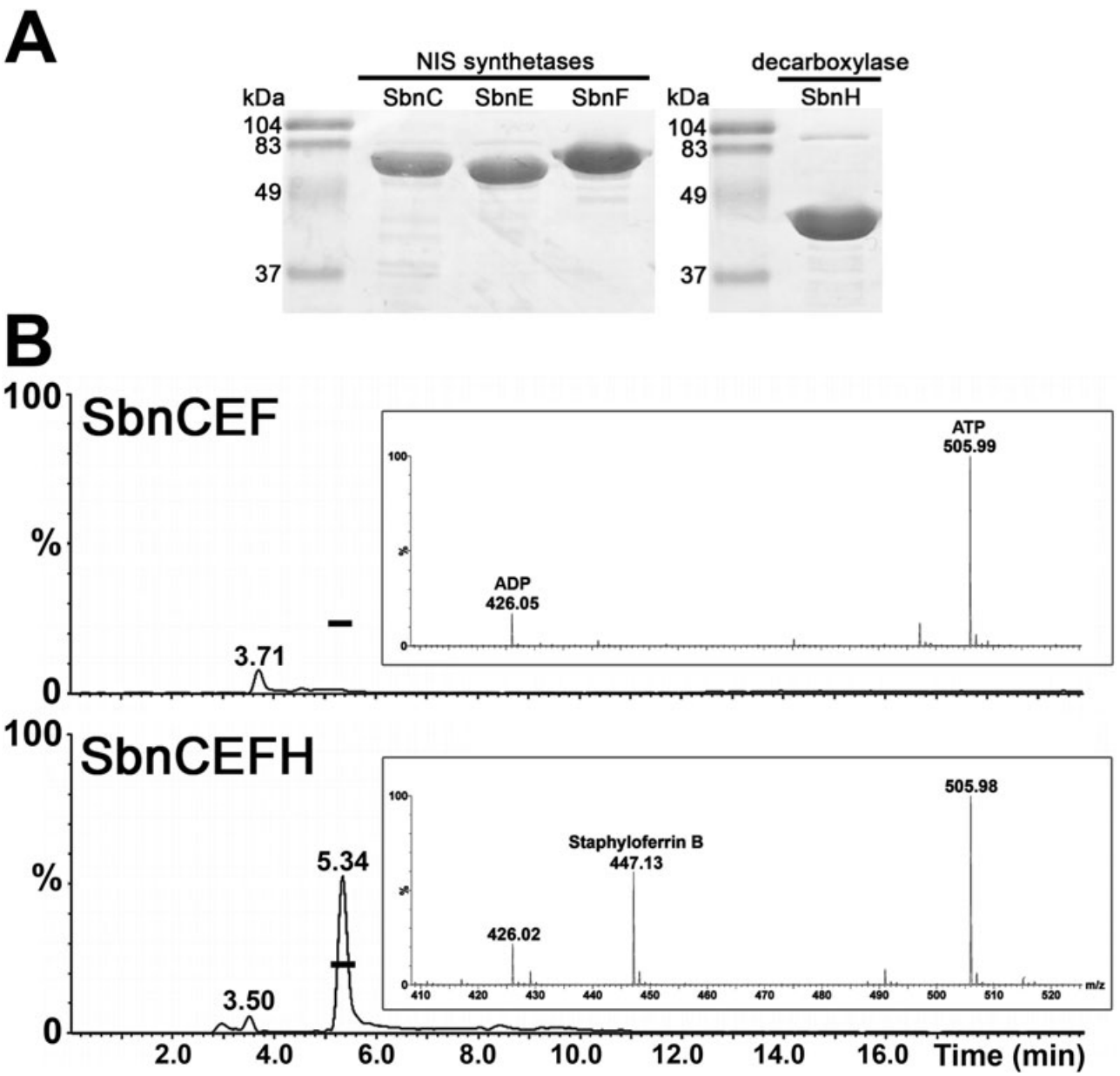

Fig. 3. Analysis of the *in vitro* synthesis of staphyloferrin B (SB).
A. SDS-polyacrylamide gel showing the purification of SbnC, SbnE, SbnF and SbnH proteins.
B. Selected ion chromatograms for the ion at *m/z* 447.1 and ESI-MS mass spectra (inset) of the region in the chromatogram shown by the black horizontal bar. Also included in the spectra are species corresponding to ATP and ADP (ATP is included in reactions at a concentration of 5 mM), which serve the purpose of internal standards. Enzyme reactions contained citrate, L-2,3-Dap, α-KG, ATP, Mg^{2+}, SbnC, SbnE, SbnF without (top panel) or with (bottom panel) inclusion of SbnH. The mass ion at *m/z* 447.1 is staphyloferrin B $[M-H]^-$, and this mass ion was not observed when any of the above-mentioned reaction components were omitted.

the activity of the SbnC, SbnE and SbnF enzymes, and to determine if they were sufficient for SB synthesis, each was independently overexpressed in *E. coli* as a hexahistidine-tagged derivative, and subsequently purified using nickel-affinity chromatography (Fig. 3A). When the three synthetases were incubated together with SB components Dap, citrate, Dae and α-KG, an ion corresponding to SB was not formed (Fig. 3B, top panel). Given the possibility that an additional Sbn enzyme was a required component in the SB biosynthetic pathway, additional purified Sbn enzymes were added to the reaction. Notably, when SbnH, a putative pyridoxal-5′-phosphate (PLP)-dependent decarboxylase, was combined in reactions with the three synthetases and substrates, an ion corresponding to that of SB was produced (Fig. 3B, bottom panel). The SB ion was not produced when any of

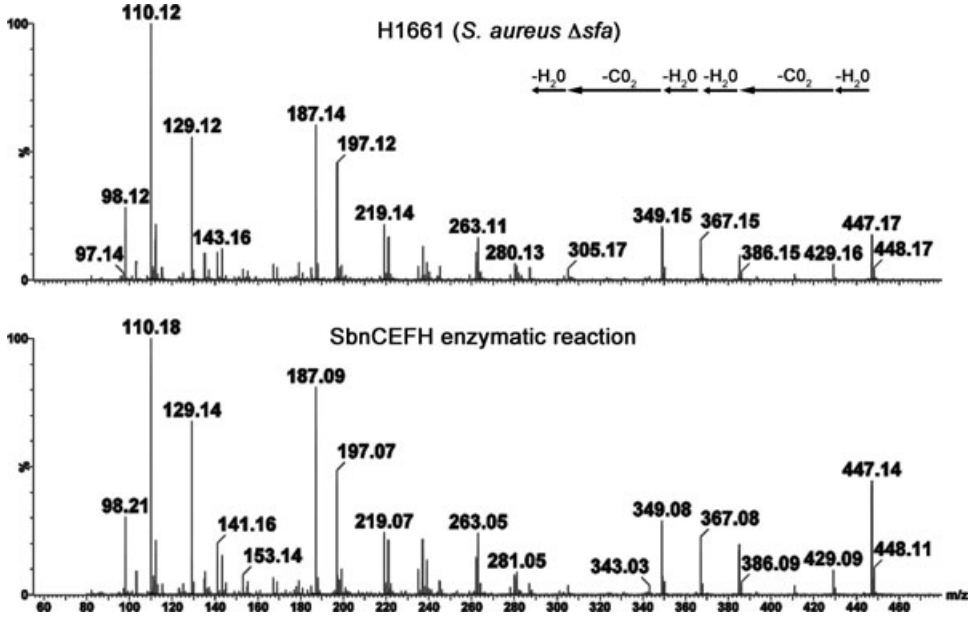

Fig. 4. ESI-MS/MS fragmentation pattern of ions at *m/z* 447.1 (staphyloferrin B) is identical between samples obtained *in vivo* [i.e. from material obtained from culture supernatants (Fig. 2, top panel)] and *in vitro* [i.e. from material synthesized *in vitro* (Fig. 3B, bottom panel)]. The $[M\text{-}H]^-$ ion fragments to give daughter ions resulting from losses of water and carbon dioxide, as indicated.

ATP, Mg^{2+}, SbnC, SbnE, SbnF, SbnH, Dap, citrate or α-KG was omitted from the reaction (data not shown). Notably, SB synthesis could proceed even without the addition of Dae in the reaction (see below for further discussion). ESI-MS/MS was used to confirm that SB produced *in vitro* was the same as that isolated from spent culture supernatants of iron-starved *S. aureus* (Fig. 4).

In vitro *synthesized staphyloferrin B is biologically active*

Having established that SB can be produced *in vitro*, it was important to show that the molecule had the same biological properties (i.e. the ability to deliver iron to bacteria) as that of SB produced by *S. aureus* cells. This was confirmed by showing that enzymatic reaction material derived from complete reactions (i.e. those containing citric acid, Dap, α-KG, ATP, Mg^{2+} and SbnCEFH; see Fig. 3), and not that derived from reactions lacking any one component (e.g. lacking ATP or one or more enzymes), could readily promote the iron-starved growth of siderophore-deficient *S. aureus* (i.e. Δ*sfa*Δ*sbn*) in a concentration-dependent fashion (Fig. 5A). This SB-dependent growth promotion was mediated by the ABC transporter SirABC (Fig. 5B), which is encoded by the *sirABC* operon divergently transcribed from the *sbn* operon (Fig. 1A).

SbnE, a citrate-desymmetrizing enzyme, initiates staphyloferrin B synthesis

Staphylococcus aureus SbnE is 578 amino acids in length with a calculated molecular mass of 66 kDa and an estimated isoelectric point (pI) of 5.52. Gel filtration analyses demonstrate that the protein exists in solution as a mixture of monomer and dimer (data not shown). Bioinformatic analyses place the enzyme in the IucA/IucC family of NIS synthetases and, more specifically, into the type A subfamily (Challis, 2005). BLAST searches demonstrate that SbnE shares significant similarity with the type A enzymes AsbA (initiates petrobactin synthesis in *Bacillus anthracis*) (Oves-Costales *et al.*, 2009) and AcsD (initiates achromobactin synthesis in *Pectobacterium chrysanthemi* and *Pseudomonas syringae*) (Berti and Thomas, 2009; Schmelz *et al.*, 2009). The type A enzymes are specific for condensation reactions involving citric acid and more importantly, a recent thorough study on AcsD from *P. chrysanthemi* showed that this enzyme catalysed the stereospecific adenylation of one of the prochiral carboxymethyl groups of citrate, which primes it for reaction with nucleophilic L-serine to form an achromobactin precursor (Schmelz *et al.*, 2009).

To assay for enzymatic activity of SbnE, the hydroxylamine trapping assay (described in Kadi and Challis, 2009) was used. Essentially, this assay is used to monitor the specific activity of a synthetase towards a particular carboxylic acid. As illustrated in Fig. 6, of the three NIS synthetases tested (SbnC, SbnE and SbnF), only SbnE showed a high level of specific activity towards citrate as a substrate. In the structure of SB (Fig. 1B), citrate is joined on either side by Dap and Dae. Liquid chromatography-electrospray ionization-mass spectrometry (LC-ESI-MS) was used to demonstrate that upon incubation with citrate and Dap, SbnE readily catalysed

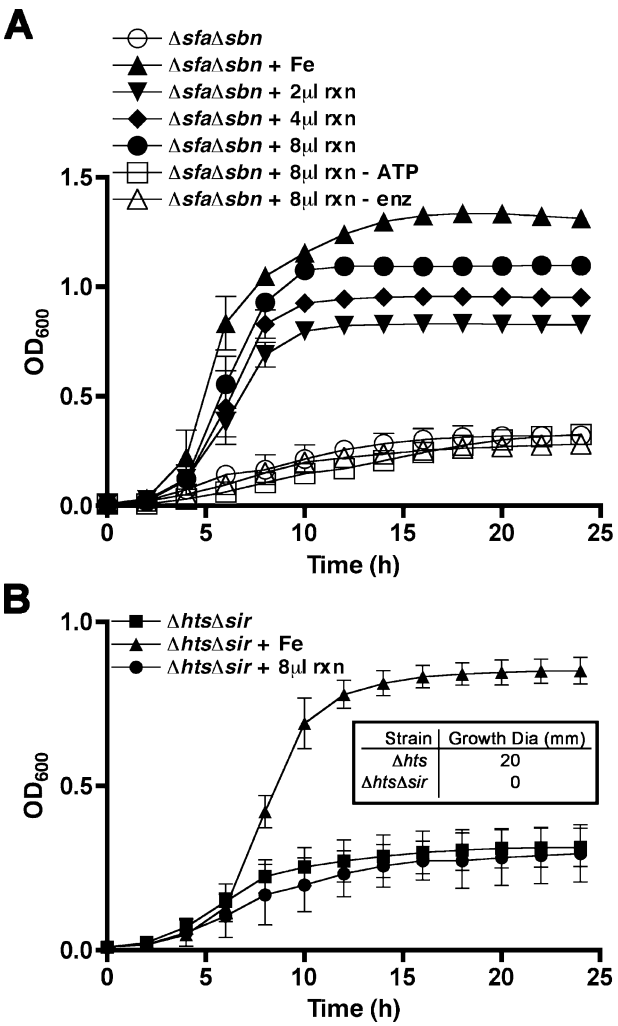

Fig. 5. *In vitro* synthesized staphyloferrin B (SB) is biologically active.
A. Increasing amounts of SB from complete reactions promoted increasing growth of iron-starved *S. aureus* Δ*sfa*Δ*sbn*, reaching levels comparable to those obtained when 50 μM $FeCl_3$ was added to culture media. Material from reactions that lacked either ATP or Sbn enzymes failed to promote growth.
B. An intact SirABC transport system (see Fig. 1A for physical map of *sir-sbn* locus) is required for SB-dependent iron acquisition observed either in liquid growth media or in siderophore plate bioassays (inset). As described in *Experimental procedures*, the SB biosynthesis reactions produced 1 nM Desferal™ equivalents of SB as determined using the CAS siderophore detection assay.
Each data point represents the mean ± SD of triplicate samples.

the ATP-dependent formation of a mass ion species of $[M\text{-}H]^-$ at *m/z* 277.1 (Fig. 7A), consistent with the formation of **[3]** (Fig. 8). This reaction product reacted strongly with CAS reagent but was unable to promote the iron-starved growth of *S. aureus* (data not shown). The SbnE-dependent condensation of citrate with Dap was further confirmed by the appearance of a mass ion at *m/z* 279.1 when citrate-2,4-$^{13}C_2$ replaced citric acid in the reaction (Fig. 7A). SbnF, which showed some activity towards citrate in hydroxylamine assays (Fig. 6), was unable to form the citryl-Dap intermediate (Fig. 7A).

The kinetics of the recognition of citrate by SbnE were determined using the hydroxylamine trapping assay, and were as follows: $K_m = 0.99$ mM ± 0.12, $V_{max} = 0.04$ mM min^{-1} ± 0.002 and $K_{cat} = 16.08$ min^{-1} ± 0.87. Michaelis–Menten kinetics were observed at substrate concentrations as high as 30 mM citrate.

It was of interest to determine if SbnE could also carry out a condensation reaction between citrate and Dae. The bottom three panels of Fig. 7B and Fig. S1 illustrate that this reaction does occur, but that when presented with equimolar concentrations of citrate, Dap and Dae, SbnE readily forms the citryl-Dap intermediate ($[M\text{-}H]^-$ at *m/z* 277.1) and virtually no mass ion species that would correlate with the formation of citryl-Dae ($[M\text{-}H]^-$ at *m/z* 233.1). Therefore, this suggests that Dap is the preferred amine substrate for SbnE.

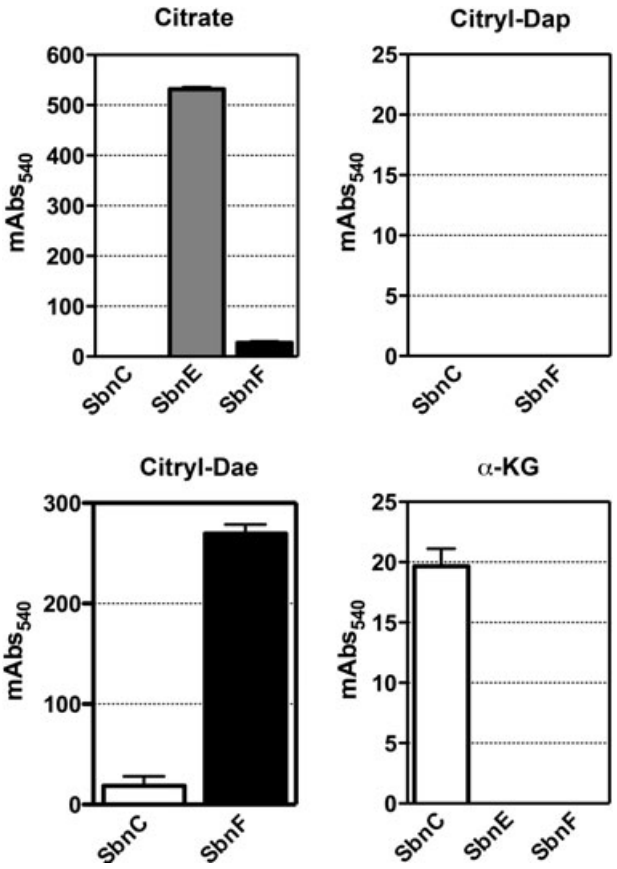

Fig. 6. Substrate specificity determination for Sbn enzymes. Sbn enzymes were mixed with carboxylic acid substrates in reactions that contained ATP, Mg^{2+} and hydroxylamine. Assays, performed according to published procedures (Kadi and Challis, 2009), detected the production of hydroxamates. Results are presented for reactions using the carboxylic acid substrates citrate, cityrl-Dap, citryl-Dae and α-KG. Citryl-Dap and citryl-Dae were prepared from reactions that contained ATP, Mg^{2+}, SbnE, citrate and either Dap or Dae respectively.

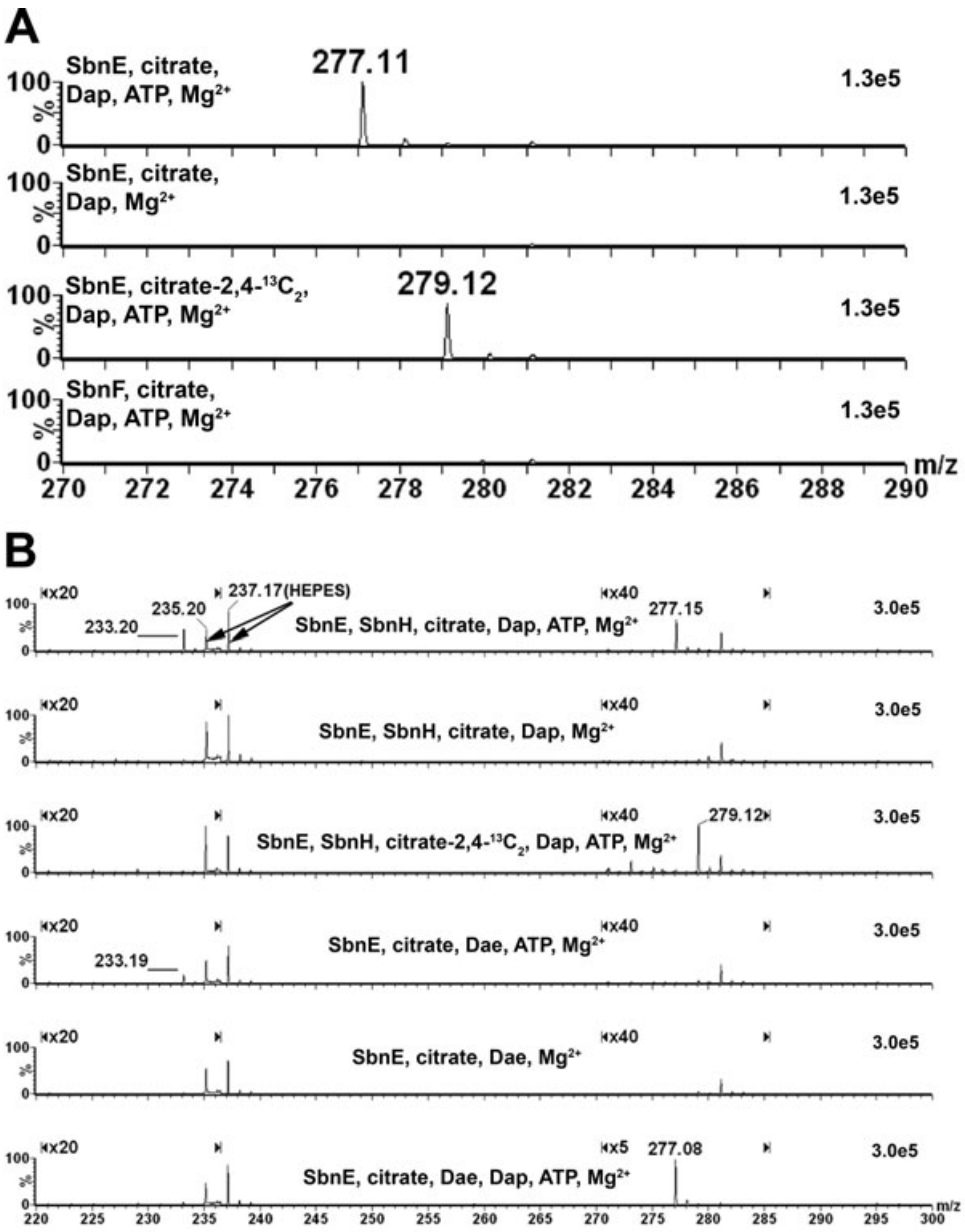

Fig. 7. LC-ESI-MS data to identify mass ions consistent with proposed staphyloferrin B biosynthetic intermediates. In each panel, MS spectra focused on mass ranges for identification of particular intermediates for the first (A), second (B), third (C) and final (D) steps in SB biosynthetic pathway, as outlined in Fig. 8. Each data set resulted from reactions run in HEPES buffer (see *Experimental procedures*) and was normalized to the intensity of a particular mass ion present in the samples (e.g. HEPES or ADP).

SbnH carries out PLP-dependent decarboxylation of the citryl-Dap intermediate

SbnH is 400 amino acids in length and has a mass of 45.8 kDa and an estimated pI of 5.85. In solution, SbnH exists as a dimer (data not shown). SbnH shares significant similarity with PLP-dependent decarboxylase enzymes, among them AscE from the achromobactin biosynthetic pathway. SbnH was overexpressed and purified from the cytoplasm of *E. coli* with an intense yellow colour which suggests a population of the enzyme exists in the PLP-bound form. As described above, our data demonstrated the *sine qua non* role of SbnH in SB synthesis. It was of interest therefore to define at which step the decarboxylation occurs in the pathway. As illustrated in Fig. 3, SB biosynthesis was dependent on the presence of substrates citric acid, Dap and α-KG, but not Dae, in the presence of SbnCEFH. This is noteworthy because theoretical decarboxylation of Dap would produce Dae. However, SbnH-dependent decarboxylation of Dap to

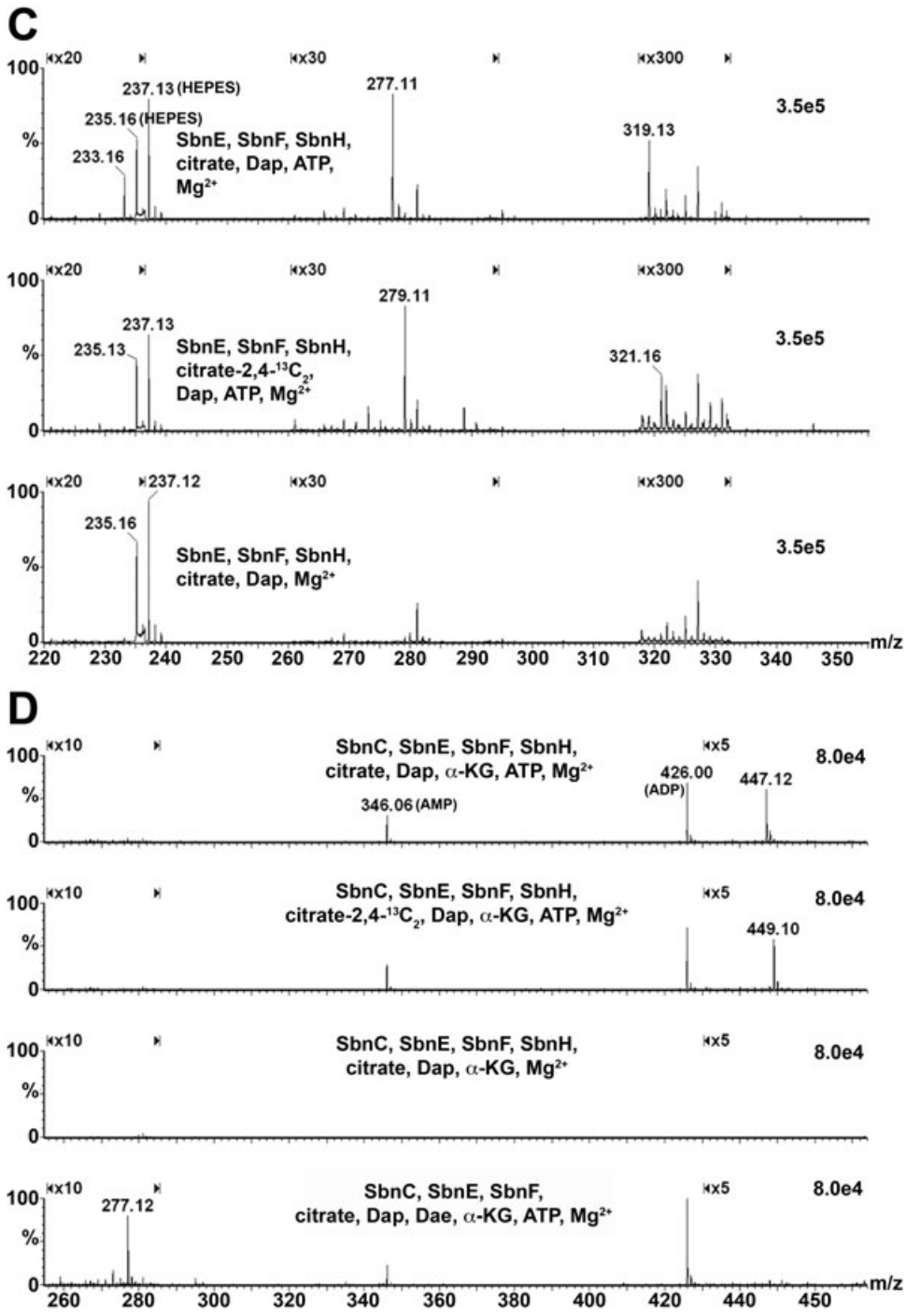

Fig. 7. *cont.*

yield free Dae as a substrate is unlikely to be a biologically relevant process since, as shown in Fig. 7B and Fig. S1, free Dae is only poorly incorporated onto citrate by SbnE, and especially in the presence of Dap. Therefore, this would indicate that decarboxylation occurs preferentially on an SB intermediate. As demonstrated in Fig. 7B and Fig. S1, when SbnH was added to reactions containing SbnE, citric acid and Dap, an $[M\text{-}H]^-$ ion at *m/z* 233.1 appeared, in agreement with a proposed decarboxylation reaction on **[3]** to yield **[4]**. In reactions where citric acid-2,4-$^{13}C_2$ replaced citric acid, the mass ion of $[M\text{-}H]^-$ at *m/z* 233.1 disappeared and was shifted up two mass units. The appearance of an SB-intermediate species at $[M\text{-}H]^-$ at *m/z* 235.1 was not obvious in reactions buffered with

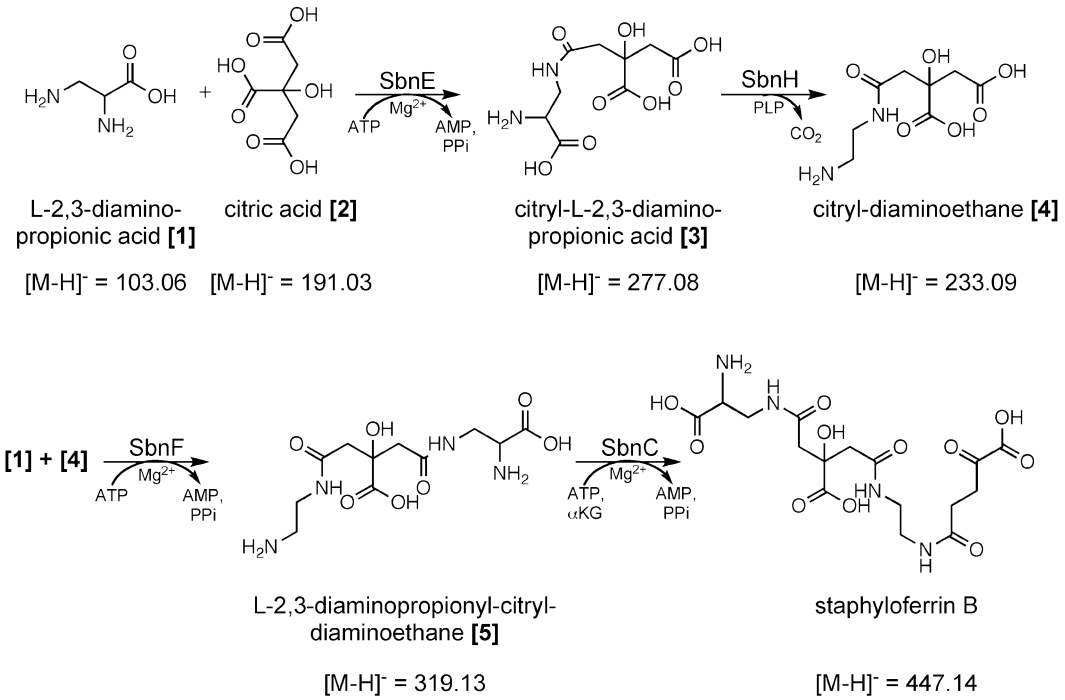

Fig. 8. Proposed scheme for the biosynthesis of staphyloferrin B. Abbreviations used: αKG, α-ketoglutarate; PLP, pyridoxal-5′-phosphate.

HEPES since it has the same mass as that of the deprotonated form of HEPES buffer (two predominant mass ions are observed for HEPES, one at 237.1 and another at 235.1) (Fig. 7B). To circumvent this problem, the reactions were also performed in phosphate buffer, pH 7.4. Using phosphate buffer, the 233.1 to 235.1 mass ion shift due to replacement of citrate with citrate-2,4-$^{13}C_2$ in the reactions is readily apparent given the absence of interfering background in this region of the spectra (Fig. S1).

SbnF is necessary to form a staphyloferrin B intermediate

SbnF is a 592-amino-acid-long protein with a theoretical mass of 68.9 kDa and an estimated pI of 5.07. Gel filtration analyses indicate that SbnF is a mixture of monomer and dimer in solution (data not shown). Bioinformatic analyses, along with the known structure of SB, indicate that SbnF, a putative type C synthetase, generates an amide bond between an amino- or hydroxyl-containing substrate and a second substrate which is already a monoamide but still possesses a free prochiral carboxyl. Thus, given that our data were consistent with the generation of **[4]** from a reaction containing SbnE, SbnH, citrate and Dap, we postulated that SbnF could act on this intermediate to add a molecule of Dap, which would be consistent with the known structure of SB (see Fig. 1). The potential substrate was first examined using substrate trapping (hydroxylamine) assays. Not surprisingly, SbnF did not react with the citryl-Dap product of a reaction containing SbnE, citrate and Dap (the mass ion at *m/z* 277.1 corresponding to **[3]**) (Fig. 6). To determine whether SbnF recognizes a citryl-Dae intermediate as a substrate in the hydroxylamine assays, we attempted to use the product of reactions containing SbnE, SbnH, citrate and Dap (which yields a mass ion of 233.1 consistent with citryl-Dae **[4]**). Unfortunately, it was determined that PLP, which is associated with SbnH, interfered with the assay. To overcome this, citryl-Dae was generated by reacting SbnE with citrate in the presence of a 17-fold molar excess Dae compared with substrate concentrations that were used for routine reactions set up for all LC-ESI-MS experiments. In this case, SbnF showed high levels of activity with the citryl-Dae intermediate (Fig. 6). In the structure of SB, the Dae molecule is linked to citrate and Dap. Therefore, it was reasonable to assume that SbnF recognized and condensed the citryl-Dae intermediate with Dap. This reaction would generate a species of $[M-H]^-$ at *m/z* 319.1. LC-MS confirmed that this species appeared in ATP-dependent reactions containing SbnE, SbnH, SbnF, citrate and Dap (Fig. 7C). Mass ions of 233.1 and 277.1 were also detectable in these reactions. When reactions contained citrate-2,4-$^{13}C_2$ in place of citrate, the *m/z* 233.1, 277.1 and 319.1 mass ions were each shifted two mass units higher (Fig. 7C). Consistent with the hydroxylamine assay results showing that SbnF did not react with the SbnE-catalysed citryl-Dap product, we could not detect a mass ion of *m/z* 363.1 (Dap-citryl-Dap)

when SbnF was reacted with SbnE, citrate and Dap (data not shown). All together, the data are consistent with SbnF acting in the pathway subsequent to SbnE and SbnH, and generating **[5]** by condensing one molecule of Dap with **[4]**.

SbnC activates α-KG in a reaction that completes the synthesis of staphyloferrin B

SbnC is 584 amino acids long with a mass of 66.4 kDa and an estimated pI of 4.93. Using gel filtration chromatography, SbnC was determined to exist in solution as a mixture of monomer and dimer (data not shown). SbnC groups with type B synthetases based on bioinformatic analyses (Challis, 2005), meaning that it putatively catalyses amide bond formation between an amino or hydroxyl group of one substrate and the C5 carboxyl group of α-KG. In agreement with this prediction, the hydroxylamine-trapping assay showed that SbnC, but not SbnE or SbnF, activates α-KG (Fig. 6). As described above (illustrated in Fig. 3), LC-ESI-MS demonstrated that reactions containing α-KG, citrate, Dap, SbnE, SbnH and SbnF (i.e. lacking SbnC) do not form SB (no mass ions of 447.1 in negative ion mode detectable above background) but do form a mass ion of *m/z* 319.1 that correlates with compound **[5]** (data not shown). As shown in Fig. 3 and again in Fig. 7D (top spectra), complete reactions (i.e. all four enzymes and three SB component substrates) readily synthesized a mass ion at *m/z* 447.1, consistent with the mass of SB. The mass of SB was two mass units heavier when citrate was replaced with citrate-2,4-$^{13}C_2$ (Fig. 7D, second spectra). The ATP dependence of the synthesis was again confirmed in the third spectra shown in Fig. 7D, as was the requirement for SbnH, even in the presence of Dae (Fig. 7D, fourth spectra). In the latter case, a build-up of the mass ion at *m/z* 277.1 was readily observed, in agreement with blockade of the pathway after the first enzymatic step (Fig. 8). Taken together, these data are consistent with the hypothesis that SbnC condenses α-KG with **[5]** in the final step of SB biosynthesis.

Discussion

Iron, or, more appropriately, its availability, plays a central role in the host–pathogen relationship. Whereas the host has developed numerous strategies to thwart pathogens by sequestering this essential nutrient, many pathogens have countered by evolving specialized iron acquisition mechanisms. *S. aureus* is a significant human and animal pathogen which has the capability to scavenge haem, doing so by releasing extracellular toxins that lyse erythrocytes, resulting in the release of haemoglobin. A specialized series of proteins (iron-regulated surface determinants) is expressed on the surface of *S. aureus*, of which the cumulative function is to affect the cell surface binding of haemoglobin and the subsequent release and transport of haem into the cell for its use in biological processes (Mazmanian *et al*., 2003; Maresso and Schneewind, 2006; Muryoi *et al*., 2008; Zhu *et al*., 2008). *S. aureus* is an interesting pathogen because not only does it acquire iron from haem, but it also produces at least two siderophores, of which the structures of SA and SB are known.

In this study, we describe the first characterization of the biosynthesis of SB, and demonstrate cell-free synthesis of SB. SB is composed of Dap, citric acid, Dae and α-KG. Given that the structure of the siderophore contains carboxylic acids and amines, it was not surprising that it would be synthesized in an NIS-dependent manner, and would likely require the activity of three NIS synthetases. The *sbn* gene cluster, which encodes three NIS synthetases (SbnCEF), was previously associated with the production of a siderophore that was not structurally elucidated (Dale *et al*., 2004a). As described here, we took advantage of *S. aureus* deletion mutants to show that strains deleted for *sfa* (i.e. do not synthesize SA) make readily detectable amounts of SB. SB synthesis in *S. aureus* was dependent on the *sbn* genes since the siderophore was not detected in culture supernatants of a mutant containing deletions of both the *sfa* and *sbn* gene clusters.

In order to elucidate the SB biosynthetic pathway, Sbn proteins were purified and reacted with SB components. It is noteworthy that inclusion of the three synthetases (SbnCEF) along with ATP, Mg^{2+} and the four component substrates of SB, in a one-pot assay, did not result in the formation of SB. SB was only formed with the inclusion in the assay of the PLP-dependent decarboxylase, SbnH. Moreover, with SbnH included in reactions, Dae as a component substrate was not required for SB synthesis to proceed. This would suggest that the essential decarboxylation step occurs on a Dap-containing intermediate (decarboxylation of Dap yields Dae) and argues against SbnH activity on the Dap substrate before its inclusion into the growing structure. The data are consistent with decarboxylation of **[3]** to yield **[4]** (Fig. 8). Although the data demonstrated that a decarboxylation step was required for SB synthesis (specifically for decarboxylation of the SbnE-derived citryl-Dap intermediate to a citryl-Dae intermediate), we could still show that SbnE was capable of directly condensing Dae with citrate, presumably bypassing the requirement for a decarboxylation step. This would be similar to data recently published on the achromobactin biosynthetic pathway (Berti and Thomas, 2009). In the biosynthesis of achromobactin, which is comprised of citrate, α-KG, ethanolamine and diaminobutyrate, the first step is the AcsD (analogous to SbnE)-dependent

condensation of citric acid with serine, and this intermediate is thought to be decarboxylated to *O*-citryl-ethanolamine. Berti and Thomas (2009) have shown that if AcsD were instead provided with citric acid and ethanolamine, the *O*-citryl-ethanolamine intermediate could be formed, thus bypassing a predicted PLP-dependent AcsE (analogous to SbnH)-mediated decarboxylation step and allowing synthesis of the complete achromobactin siderophore structure. In contrast, in the SB pathway, we have shown that a decarboxylation step is required for SB synthesis and, presumably, as a result of our data indicating that SbnE strongly favours condensation of citrate with Dap as opposed to Dae (Fig. 7D). Since another molecule of Dap is required to form the final structure, it is impossible to bypass the requirement for Dap in the synthesis of SB. Moreover, the *in vivo* concentration of Dap is likely to be higher than that of Dae, especially since we have evidence that the SbnA and SbnB enzymes synthesize Dap (F.C. Beasley, J. Cheung and D.E. Heinrichs, unpubl. obs.) as a method to ensure the presence of this precursor.

An important difference between the achromobactin and SB pathways is the lack of processive addition of α-KG to the structure of SB by a type B enzyme (SbnC for SB and AcsA for achromobactin). It has been observed that two successive α-KG molecules are condensed onto the achromobactin intermediate by AcsA to form the final siderophore, provided that the serine in the α-ketoglutaryl-diaminobutryl-citryl-serine intermediate has been decarboxylated prior to addition of the second α-KG (Berti and Thomas, 2009). It is possible in this case that the carboxyl group on serine acts as a steric obstacle preventing AcsA from adding another α-KG to the intermediate. By comparing this observation with the known structure of SB (Fig. 8) we can make the analogy that the presence of the carboxyl group on Dap is similarly inhibiting SbnC from processively adding a second α-KG to the SB structure. This is yet another interesting difference in SB because we have shown in this study that the decarboxylation event by SbnH occurs on **[3]** in order for SbnF to recognize it as a substrate (Fig. 7B and C). Even when all four enzymes were incubated with citrate, Dap, α-KG, Mg^{2+} and ATP, we were unable to observe a mass ion that corresponded to a mass of SB, decarboxylated and condensed with another molecule of α-KG ($[M-H]^-$ at *m/z* 531) by LC-ESI-MS (data not shown). Therefore, SbnH is unable to decarboxylate the Dap on either **[5]** or the full SB structure to generate another Dae moiety that might serve as an adequate nucleophile for a condensation with a second α-KG.

Challis (2005) used bioinformatics to propose that NIS synthetases fall into three basic types (A, B and C), grouped according to specificity for particular carboxylic acids. In this study, we have demonstrated that SbnE has type A NIS activity, SbnC has type B NIS activity and SbnF has type C NIS activity, as predicted by the phylogenetic analyses, thus demonstrating the general robustness of the bioinformatic-based predictions. To date, of the close to 100 NIS synthetase enzymes identified through genome mining, only a few have been biochemically characterized (Kadi *et al*., 2008; Oves-Costales *et al*., 2008; 2009; Schmelz *et al*., 2009). The SB pathway is interesting to study because it uses a representative of each of the three synthetase types, thus representing a good model system to study. Cotton *et al*. have recently shown that the two type A NIS synthetases in the SA pathway cluster with the type B NIS synthetases, thus forming a new subtype of enzymes with A-type chemistry (Cotton *et al*., 2009) and highlighting the need for continued biochemical studies of these important enzymes to elucidate their activity.

In a recent landmark study, Schmelz *et al*. (2009) defined a high-resolution crystal structure of the type A NIS enzyme AcsD from *P. chrysanthemi*. They provided important insight into the mechanism of action of this family of proteins by observing the acyladenylate intermediate that is formed during activation of one of the prochiral carboxylate groups of citrate. Subsequent attack by an amine nucleophile (L-serine in the case of AcsD) results in a condensation reaction and release of the citryl-L-serine siderophore intermediate. This points out a key difference between NIS and NRPS systems. In the latter, intermediate structures remain associated with the modular synthetic machinery. In the case of the former, one might suspect that protein:protein (i.e. synthetase:synthetase) interactions may be involved that would ensure greater efficiency in the synthesis of the siderophore molecule, in light of the fact that intermediate structures are freely dissociable from the NIS synthetases. The possible existence of higher-order protein complexes for these biosynthetic pathways remains to be determined.

This study adds to the recent and rapid progress in our understanding the function of NIS synthetases, an important class of bacterial enzymes. We demonstrate, for the first time, the *in vitro* synthesis of biologically active SB by combining three synthetases and a decarboxylase in one-pot enzyme reactions, and propose a biosynthetic pathway. This is an important step towards more detailed mechanistic and structural studies on the synthetases and their reaction products.

Experimental procedures

Bacterial strains, plasmids and standard growth conditions

Bacterial strains and plasmids used in this study are described in Table 1. *E. coli* were grown in Luria-Bertani broth (Difco). For experiments not directly involved in the analysis of iron uptake, *S. aureus* were grown in tryptic soy broth

Table 1. Bacterial strains, plasmids and oligonucleotides used in this study.

Bacterial strains, plasmids and oligonucleotides	Description[a]	Source or reference
E. coli		
DH5α	F⁻ ϕ80 dL*acZ*ΔM15 *recA1 endA1 nupG gyrA96 glnV44 thi*-1 *hsdR17*(r_K^- m_K^+) λ⁻*supE44 relA1 deoR* Δ(*lacZYA-argF*)U169	Promega
ER2566	F⁻ λ⁻ *fhuA2* [*lon*] *ompT lacZ*::T7 gene 1 *gal sulA11* Δ(*mcrC-mrr*)114::IS*10* R(*mcr*-73::miniTn*10*-Tet^S)2 R(*zgb*-210::Tn*10*)1 (Tet^S) *endA1* [*dcm*]	New England Biolabs
BL21(DE3)	F⁻ *ompT gal dcm lon hsdS$_B$* (r_B^- m_B^-) λ(DE3 [*lacI lacUV5*-T7 gene 1 *ind1 sam7 nin5*])	Novagen
S. aureus		
RN4220	r_K^- m_K^+ accepts foreign DNA	Kreiswirth *et al.* (1983)
RN6390	Prophage-cured wild-type strain	Peng *et al.* (1988)
H306	RN6390 *sirA*; Km^R	Dale *et al.* (2004b)
H1324	RN6390 Δ*sbn*; Tet^R	Beasley *et al.* (2009)
H1661	RN6390 Δ*sfa*; Km^R	Beasley *et al.* (2009)
H1649	RN6390 Δ*sbn* Δ*sfa*; Tet^R Km^R	Beasley *et al.* (2009)
H1448	RN6390 Δ*hts*; Tet^R	Beasley *et al.* (2009)
H1480	RN6390 *sirA* Δ*hts*; Tet^R Km^R	Beasley *et al.* (2009)
Plasmids		
pET28a(+)	Overexpression vector for hexahistidine-tagged proteins; Km^R	Novagen
pSbnC	pET28a(+) derivative encoding SbnC; Km^R	This study
pSbnE	pET28a(+) derivative encoding SbnE; Km^R	This study
pSbnF	pET28a(+) derivative encoding SbnF; Km^R	This study
pSbnH	pET28a(+) derivative encoding SbnH; Km^R	This study

a. Km, Kanamycin; Tet, tetracycline.

(Difco). Tris-minimal succinate (TMS) was prepared as described (Sebulsky *et al.*, 2004) and used as an iron-limited minimal medium. To further restrict the level of free iron in TMS, the iron-chelating compounds 2,2′-dipyridyl and ethylene diamine-di(*o*-hydroxyphenol acetic acid) (EDDHA) were added as indicated in the text. Where necessary, kanamycin (30 μg ml^{-1}) was incorporated into media for the growth of *E. coli* strains. For *S. aureus*, kanamycin (50 μg ml^{-1}), neomycin (50 μg ml^{-1}) and tetracycline (4 μg ml^{-1}) were incorporated into growth media as required. Solid media were obtained by the addition of 1.5% (w/v) Bacto agar (Difco). All bacterial growth was conducted at 37°C unless otherwise stated. Iron-free water for preparation of growth media and solutions was obtained by passage through a Milli-Q water filtration system (Millipore Corp.).

Recombinant DNA methodology

Standard DNA manipulations were performed essentially as described by Sambrook *et al.* (1989). Restriction endonucleases and DNA-modifying enzymes were purchased from Roche Diagnostics (Laval, Quebec, Canada), New England Biolabs (Mississauga, Ontario, Canada), Life Technologies (Burlington, Ontario, Canada) and MBI Fermentas (Flamborough, Ontario, Canada). Plasmid DNA was purified using QIAprep plasmid spin columns (QIAgen, Santa Clarita, California) as described by the manufacturer. Polymerase chain reactions were performed using *Pwo*I DNA polymerase (Roche Diagnostics).

Siderophore plate bioassays

Siderophore plate bioassays were performed as described (Beasley *et al.*, 2009). Growth promotion, as measured by the diameter of the growth halo around each disk, was determined after 36 h incubation at 37°C.

Bacterial growth curves

Bacteria were cultured for 12 h in TMS broth then 12 h in TMS broth containing 100 μM 2,2′-dipyridyl (Sigma-Aldrich). Cells were washed twice in saline, and diluted 1:100 into 60% horse serum (Sigma-Aldrich)–40% TMS broth. For iron-replete media, 50 μM $FeCl_3$ was included. Cultures were grown under constant, medium-amplitude shaking in a Bioscreen C machine (Growth Curves, USA). Optical density was measured at 600 nm every 30 min. However, for clarity of growth curve figures, data are shown only at 2 h intervals.

Siderophore detection

To measure levels of siderophore activity, chrome azurol S (CAS) shuttle solution (Schwyn and Neilands, 1987) was prepared. In the case of *in vitro* synthesized SB, 50 μl of the reaction mixture was removed and diluted in 450 μl of deionized water followed by 500 μl of CAS shuttle solution in a 1 ml spectrophotometer cuvette. The mixture was then incubated in the dark for 45 min. Siderophore quantification and absorbance readings were performed as described (Beasley *et al.*, 2009).

Protein overexpression and purification

Proteins were expressed in *E. coli* BL21(DE3) by cloning the coding regions, amplified from the genome of *S. aureus* Newman, into pET28a(+). *E. coli* cells containing expression

constructs were grown to mid-log phase at 37°C with aeration before IPTG (isopropyl-β-D-thiogalactopyranoside) (0.5 mM) was added, and cells cultured for an additional 16 h at room temperature. The cells were re-suspended in 50 mM HEPES buffer (pH 7.4), 500 mM NaCl, 10 mM imidazole and lysed in a French pressure cell at 10 000 psi, and the lysate was centrifuged at 15 000 *g* for 15 min to remove unbroken cells and debris, prior to centrifugation at 150 000 *g* for 60 min to remove insoluble material. The soluble sample was applied to a 1 ml HisTrap nickel affinity (GE Healthcare) column equilibrated with buffer A and the 6xHis-tagged proteins were eluted from the column with a gradient of 0–80% buffer B over 20 column volumes; buffer A contained 50 mM HEPES buffer (pH 7.4), 500 mM NaCl, 10 mM imidazole, and buffer B contained 50 mM HEPES buffer (pH 7.4), 500 mM NaCl, 500 mM imidazole. Proteins were dialysed into 50 mM HEPES (pH 7.4), 150 mM NaCl and 10% glycerol at 4°C. Protein purity was confirmed using ESI-MS and sodium dodecyl sulphate-polyacrylamide gel electrophoresis (Sambrook *et al*., 1989). Protein yield from the induced cultures harbouring the expression constructs was determined to be 3 mg l^{-1} (SbnC), 3 mg l^{-1} (SbnE), 3 mg l^{-1} (SbnF) and 17 mg l^{-1} (SbnH).

Mass spectrometry

LC-MS and LC-MS/MS analyses of concentrated culture supernatant samples were performed as described previously (Beasley *et al*., 2009).

For analysis of *in vitro* reaction products, enzymes were first removed using centricon with molecular weight cut-off of 10 000. Effluent was injected onto the LC-MS/MS system, consisting of a Waters CapLC with a Phenomenex Jupiter Proteo 90 A column (150 × 1.0 mm, 4 μm) coupled to a Q-TOF (micro, Waters) mass spectrometer. Separation was carried out at a flow rate of 40 μl min^{-1} with a gradient starting at 1% B and increase to 50% B in 15 min and then to 95% B in 5 min, and hold for 5 min. Solvent A was water and solvent B was 95% acetonitrile, both with 0.1% formic acid. LC-ESI-MS analysis was performed in negative ion mode with a scan range of 200–700 *m/z*. Collision-induced dissociation was performed with a mass range of 60–500 *m/z* using argon as the collision gas. Variable collision energy of 20–30 V was applied to obtain an informative fragmentation spectrum. Data were acquired and analysed by MassLynx 4.0 (Micromass).

In vitro *staphyloferrin B biosynthesis*

Reactions, in a total volume of 100 μl, consisted of 5 mM ATP, 0.5 mM $MgCl_2$, 0.5 mM pyridoxal-5′-phosphate, 1 mM Dap HCl, 1 mM sodium citrate, 1 mM α-KG, 5 μM SbnC, 5 μM SbnE, 5 μM SbnF, 5 μM SbnH and was buffered in 50 mM HEPES pH 7.4. HEPES was replaced with 50 mM phosphate buffer pH 7.4 for some reactions where ion species from HEPES interfered with detection of a SB intermediate at *m/z* 235. When assessing the ability of Dae to substitute the need for SbnH, 1 mM Dae was added to replace the SbnH and pyridoxal-5′-phosphate components of the above reaction mixture. Reactions were incubated overnight at room temperature in the dark. The complete reaction resulted in the production of 1 nM Desferal™ equivalents as determined using the CAS siderophore detection assay.

Substrate selectivity (hydroxamate formation) assays

All reactions were performed in 300 μl volumes and the following were common to each reaction: 2.25 mM ATP, 15 mM $MgCl_2$, 150 mM hydroxylamine and 50 mM HEPES pH 7.4. To assess which enzyme utilized citrate as a substrate, 5 μM SbnC, SbnE or SbnF was incubated with 3 mM citrate and the common reaction components as described above. Similarly, to assess which enzyme utilized α-KG as a substrate, 5 μM SbnC, SbnE or SbnF was incubated with 3 mM α-KG and the common reaction components. To assess the potential recognition of citryl-Dae as a substrate by SbnF or SbnC, this intermediate was formed in overnight reactions containing 2.25 mM ATP, 15 mM $MgCl_2$, 3 mM sodium citrate, 50 mM Dae, 5 μM SbnE buffered in 50 mM HEPES pH 7.4. This reaction was then heat treated at 70°C to deactivate SbnE and the reaction was then centrifuged at 20 000 *g* for 10 min to pellet precipitated enzyme. The supernatant which now contains the citryl-Dae intermediate was incubated with fresh 5 μM SbnF or SbnC, 2.25 mM ATP and 150 mM hydroxylamine. To assess the potential recognition of citryl-Dap as a substrate for SbnF or SbnC, this intermediate was formed as described above except that Dae was replaced with 50 mM Dap instead. For each reaction, a duplicate control reaction was prepared in which the enzyme was previously inactivated by heating at 100°C for 10 min. All reactions described above were incubated at room temperature in the dark for 1 h before addition of 300 μl of stopping solution which consisted of 10% (w/v) $FeCl_3$ and 3.3% (w/v) trichloroacetic acid in 0.7 M HCl. Reactions were centrifuged at 20 000 *g* for 5 min to remove precipitate and the formation of ferric hydroxamate was detected spectrophotometrically at 540 nm. Relative absorbance values reported in this study were calculated by subtracting the absorbance of the control (boiled enzyme) reactions from the absorbance of experimental reactions.

Determination of SbnE kinetics

Determination of extinction coefficient for citryl-hydroxamate. A series of reactions, incubated overnight and containing 2.25 mM ATP, 15 mM $MgCl_2$, 150 mM hydroxylamine, 50 mM HEPES pH 7.4 and 5 μM SbnE, were tested against a range of sodium citrate concentrations ranging from 100 μM to 30 mM. After addition of stopping solution and measurement of absorbance at 540 nm, a linear relationship between absorbance and concentration of sodium citrate was established. The extinction coefficient of the citryl-hydroxamate was determined to be 0.45 mM^{-1} cm^{-1}. This extinction coefficient is similar to that which was obtained for the citrate-specific AcsD enzyme (achromobactin biosynthesis) from *P. syringae* pv. syringae B728a (Berti and Thomas, 2009).

Determination of K_m, V_{max} and K_{cat}. To determine the kinetic parameters of SbnE catalysis, 500 μM citrate was incubated

with 2.25 mM ATP, 15 mM $MgCl_2$, 150 mM hydroxylamine, 50 mM HEPES pH 7.4 and 3 μM SbnE and the resulting product conversion rate was still linear at 10 min and gave an approximately 14% substrate-to-product conversion. Therefore, reaction rates were measured spectrophotometrically at the 10 min time point with citrate concentrations ranging from 0.25 to 30 mM. Reaction rate values at each citrate concentration were fitted to the Michaelis–Menten equation and analysed by non-linear regression. Due to the limit of detection and instability of the hydroxamate product formed by SbnC, we were unable to evaluate the kinetic parameters for this enzyme. This phenomenon has been previously observed (Berti and Thomas, 2009).

Computer analyses

DNA sequence analysis and polymerase chain reaction oligonucleotide primer design were performed using Vector NTI Suite (Informax) and MacVector software packages. Graphpad Prism was used for data analysis and graphing applications.

Acknowledgements

This work was supported by an operating grant from the Natural Sciences and Engineering Research Council (NSERC) of Canada to D.E.H. J.C. was supported by an NSERC Canada Graduate Scholarship and F.C.B. was supported by a studentship from the Ontario Graduate Scholarship programme. The authors are grateful to Sung Ho Um for technical assistance.

References

Barry, S.M., and Challis, G.L. (2009) Recent advances in siderophore biosynthesis. *Curr Opin Chem Biol* **13:** 205–215.

Beasley, F.C., Vines, E.D., Grigg, J.C., Zheng, Q., Liu, S., Lajoie, G.A., *et al.* (2009) Characterization of staphyloferrin A biosynthetic and transport mutants in *Staphylococcus aureus*. *Mol Microbiol* **72:** 947–963.

Berti, A.D., and Thomas, M.G. (2009) Analysis of achromobactin biosynthesis by *Pseudomonas syringae* pv. *syringae* B728a. *J Bacteriol* **191:** 4594–4604.

Bhatt, G., and Denny, T.P. (2004) *Ralstonia solanacearum* iron scavenging by the siderophore staphyloferrin B is controlled by PhcA, the global virulence regulator. *J Bacteriol* **186:** 7896–7904.

Challis, G.L. (2005) A widely distributed bacterial pathway for siderophore biosynthesis independent of nonribosomal peptide synthetases. *Chembiochem* **6:** 601–611.

Cotton, J.L., Tao, J., and Balibar, C.J. (2009) Identification and characterization of the *Staphylococcus aureus* gene cluster coding for staphyloferrin A. *Biochemistry* **48:** 1025–1035.

Crosa, J.H., and Walsh, C.T. (2002) Genetics and assembly line enzymology of siderophore biosynthesis in bacteria. *Microbiol Mol Biol Rev* **66:** 223–249.

Dale, S.E., Doherty-Kirby, A., Lajoie, G., and Heinrichs, D.E. (2004a) Role of siderophore biosynthesis in virulence of *Staphylococcus aureus*: identification and characterization of genes involved in production of a siderophore. *Infect Immun* **72:** 29–37.

Dale, S.E., Sebulsky, M.T., and Heinrichs, D.E. (2004b) Involvement of SirABC in iron-siderophore import in *Staphylococcus aureus*. *J Bacteriol* **186:** 8356–8362.

Drechsel, H., Freund, S., Nicholson, G., Haag, H., Jung, O., Zähner, H., and Jung, G. (1993) Purification and chemical characterization of staphyloferrin B, a hydrophilic siderophore from staphylococci. *Biometals* **6:** 185–192.

Haag, H., Fiedler, H.P., Meiwes, J., Drechsel, H., Jung, G., and Zähner, H. (1994) Isolation and biological characterization of staphyloferrin B, a compound with siderophore activity from staphylococci. *FEMS Microbiol Lett* **115:** 125–130.

Kadi, N., and Challis, G.L. (2009) Chapter 17. Siderophore biosynthesis a substrate specificity assay for nonribosomal peptide synthetase-independent siderophore synthetases involving trapping of acyl-adenylate intermediates with hydroxylamine. *Methods Enzymol* **458:** 431–457.

Kadi, N., Arbache, S., Song, L., Oves-Costales, D., and Challis, G.L. (2008) Identification of a gene cluster that directs putrebactin biosynthesis in *Shewanella* species: PubC catalyzes cyclodimerization of *N*-hydroxy-*N*-succinylputrescine. *J Am Chem Soc* **130:** 10458–10459.

Konetschny-Rapp, S., Jung, G., Meiwes, J., and Zähner, H. (1990) Staphyloferrin A: a structurally new siderophore from staphylococci. *Eur J Biochem* **191:** 65–74.

Kreiswirth, B.N., Lofdahl, S., Bentley, M.J., O'Reilly, M., Schlievert, P.M., Bergdoll, M.S., and Novick, R.P. (1983) The toxic shock syndrome exotoxin structural gene is not detectably transmitted by a prophage. *Nature* **305:** 709–712.

de Lorenzo, V., and Neilands, J.B. (1986) Characterization of *iucA* and *iucC* genes of the aerobactin system of plasmid ColV-K30 in *Escherichia coli*. *J Bacteriol* **167:** 350–355.

Maresso, A.W., and Schneewind, O. (2006) Iron acquisition and transport in *Staphylococcus aureus*. *Biometals* **19:** 193–203.

Mazmanian, S.K., Skaar, E.P., Gaspar, A.H., Humayun, M., Gornicki, P., Jelenska, J., *et al.* (2003) Passage of heme-iron across the envelope of *Staphylococcus aureus*. *Science* **299:** 906–909.

Meiwes, J., Fiedler, H.-P., Haag, H., Zähner, H., Konetschny-Rapp, S., and Jung, G. (1990) Isolation and characterization of staphyloferrin A, a compound with siderophore activity from *Staphylococcus hyicus* DSM 20459. *FEMS Microbiol Lett* **67:** 201–206.

Miethke, M., and Marahiel, M.A. (2007) Siderophore-based iron acquisition and pathogen control. *Microbiol Mol Biol Rev* **71:** 413–451.

Muryoi, N., Tiedemann, M.T., Pluym, M., Cheung, J., Heinrichs, D.E., and Stillman, M.J. (2008) Demonstration of the iron-regulated surface determinant (Isd) heme transfer pathway in *Staphylococcus aureus*. *J Biol Chem* **283:** 28125–28136.

Oves-Costales, D., Kadi, N., Fogg, M.J., Song, L., Wilson, K.S., and Challis, G.L. (2007) Enzymatic logic of anthrax stealth siderophore biosynthesis: AsbA catalyzes ATP-dependent condensation of citric acid and spermidine. *J Am Chem Soc* **129:** 8416–8417.

Oves-Costales, D., Kadi, N., Fogg, M.J., Song, L., Wilson, K.S., and Challis, G.L. (2008) Petrobactin biosynthesis: AsbB catalyzes condensation of spermidine with *N*8-citryl-spermidine and its *N*1-(3,4-dihydroxybenzoyl) derivative. *Chem Commun (Camb)* (34)**:** 4034–4036.

Oves-Costales, D., Song, L., and Challis, G.L. (2009) Enantioselective desymmetrisation of citric acid catalysed by the substrate-tolerant petrobactin biosynthetic enzyme AsbA. *Chem Commun (Camb)* (11)**:** 1389–1391.

Peng, H.L., Novick, R.P., Kreiswirth, B., Kornblum, J., and Schlievert, P. (1988) Cloning, characterization, and sequencing of an accessory gene regulator (*agr*) in *Staphylococcus aureus*. *J Bacteriol* **170:** 4365–4372.

Sambrook, J., Fritsch, E.F., and Maniatis, T. (1989) *Molecular Cloning. A Laboratory Manual*. Cold Spring Harbor, NY: Cold Spring Harbor Laboratory Press.

Schmelz, S., Kadi, N., McMahon, S.A., Song, L., Oves-Costales, D., Oke, M., *et al.* (2009) AcsD catalyzes enantioselective citrate desymmetrization in siderophore biosynthesis. *Nat Chem Biol* **5:** 174–182.

Schwyn, B., and Neilands, J.B. (1987) Universal chemical assay for the detection and determination of siderophores. *Anal Biochem* **160:** 47–56.

Sebulsky, M.T., Speziali, C.D., Shilton, B.H., Edgell, D.R., and Heinrichs, D.E. (2004) FhuD1, a ferric hydroxamate-binding lipoprotein in *Staphylococcus aureus*: a case of gene duplication and lateral transfer. *J Biol Chem* **279:** 53152–53159.

Zhu, H., Xie, G., Liu, M., Olson, J.S., Fabian, M., Dooley, D.M., and Lei, B. (2008) Pathway for heme uptake from human methemoglobin by the iron-regulated surface determinants system of *Staphylococcus aureus*. *J Biol Chem* **283:** 18450–18460.

Supporting information

Additional supporting information may be found in the online version of this article.

Please note: Wiley-Blackwell are not responsible for the content or functionality of any supporting materials supplied by the authors. Any queries (other than missing material) should be directed to the corresponding author for the article.

